Al-Mustansiriyah Journal of Science
ISSN: 1814-635X (print), ISSN:2521-3520 (online) Volume 33, Issue 2, 2022 DOI: http://doi.org/10.23851/mjs.v33i2.1120

Research Article **Open Access**

The Improvement of Structural and Optical Properties of WO_3 Nanoparticles by Regulation Substrate-Target Distance in Pulsed Laser Deposition Technique

Ali Jaafar Hwaidi, Nadheer Jassim Mohammed*

Department of Physics, College of Science, Mustansiriyah University, Baghdad, IRAQ.

*Correspondent contact: nadheerphys@uomustansiriyah.edu.iq

Article Info

Received
22/12/2021

Accepted
14/02/2022

Published
30/06/2022

ABSTRACT

Pulsed laser deposition technique has been employed to prepare thin films of WO_3 nanoparticles on a glass substrate at 400K under vacuum (1 mbar) by the increasing of the substrate-target distance in the range of about (0.5, 1.5, 2.5 and 3.5 cm). X-Ray diffraction (XRD), Scanning electron microscopy (SEM), Atomic force microscopy (AFM) and UV-Visible investigations have been observed the effect of substrate-target distance on the structural and optical properties of WO_3 nanoparticles thin films. Calculations of the transmittance data for all films were given the evidence to increase the optical bandgap values in the range (3.082, 3.046, 3.062and 3.105eV) when increasing the distance between the target and substrate in the range (0.5, 1.5, 2.5, and 3.5 cm), respectively.

KEYWORDS: Pulsed laser deposition; optical properties; tungsten oxide; absorbance; gas sensor.

الخلاصة

تم استخدام تقنية الترسيب بالليزر النبضي لتحضير أغشية رقيقة من جسيمات WO_3 النانوية على ركيزة زجاجية عند درجة حرارة 400 كلفن تحت فراغ (1 ملي بار) عن طريق زيادة المسافة بين الركيزة- الهدف في حدود حوالي (0.5 , 1.5 , 2.5 و 3.5 سم). فحوصات حيود الأشعة السينية (XRD) ، المجهر الالكتروني الماسح (SEM) ، مجهر القوة الذرية (AFM) والأشعة فوق البنفسجية المرئية (UV-Vis) اظهرت تأثير المسافة بين الهدف والركيزة على الخصائص التركيبية والبصرية لأغشية جسيمات **WO_3** النانوية الرقيقة.. بينت حسابات النفاذية لجميع الاغشية الدليل على زيادة قيم فجوة الطاقة البصرية في النطاق (3.082 , 3.046 ,3.062 و 3.107 الكترون فولت) عند زيادة المسافة بين الهدف والركيزة في المدى (0.5, 1.5, 2.5 و 3.5 سم))، على التوالي.

INTRODUCTION

Tungsten oxide (WO_3) is a semiconductor metallic oxide with a bandgap of (2.6–3.0 eV), which has been extensively studied because of various distinctive properties, such as electrochromism, photochromism, gas sensing, thermoelectric and catalytic properties [1,2]. It has potential applications in smart windows, electronic information displays, electrochromic devices, gas sensors and photocatalysts, photovoltaic devices, and photoelectrochemical devices [3]. With a very high work function of about 6.2 eV and high transparency in the visible region. Tungsten oxide has been recently applied in hybrid organic–inorganic optoelectronic devices as efficient hole (for WO_3) and electron (for WO_3-X) injection/transport layer [4, 5]. So far, various deposition techniques have been developed to prepare WO_3 films with different morphologies, crystallinity and structure, such as chemical vapor deposition [6,7], pulsed laser deposition [8], spray pyrolysis [9], electrodeposition [10], spin coating [11], sol-gel methods [12], sputtering [13], and the evaporation technique [14]. Amongst those methods, the pulse laser deposition technique has been considered largely for the growth of device quality films, and is promising in preparing WO_3 films over the classical deposition methods due to its several advantages, including low deposition temperature, good adhesion to the substrate, reproducibility and controllability of stoichiometry and crystal structure, and the easy deposition of alloys and compounds of materials with different vapor pressures. The microstructure, composition, morphology and physical properties of the several material films deposited by PLD strongly depending on the synthesis process and the

deposition conditions, e.g., substrate temperature and power density [15, 16]. Precisely stoichiometric tungsten oxide thin films have been synthesized utilizing pulsed laser deposition in a few published papers [17, 18]. However, there are few reports on plasma behavior in various substrate positions. In the present study will be focusing on the influence of substrate-target distance D_{s-t} on the structural and optical properties of the WO_3NPs thin films prepared by the pulsed laser deposition technique.

EXPERIMENTAL PART

The ceramic WO_3 target used is a pellet with dimensions (2*0.3 cm), density (3.66 g/cm^3), and purity (99.99%). It is produced by pressing squeeze at (13 ton) and sintering WO_3 powder under vacuum at 400K for 3hrs. It is a suitable target for PLD since it is dense and flat, enabling uniform energy transfer to its surface and the absence of voids keeps large particles being ejected from the surface. WO_3 NPs films were prepared by pulsed laser deposition system of WO_3 pellet fixed to a target holder located at different locations and parallel to the substrate surface. The PLD was carried out by using a Q- switched ND: YAG laser with wavelength (1064 nm), number shots of laser (1000), the substrate-target distances D_{s-t} are (0.5, 1.5, 2.5, 3.5 cm), laser flounce (5.57 J/cm^2) and spot diameter (d=3mm) at an angle of (45^o). The repetition rate of the laser beam was (5 Hz). The target and substrate were rotated at (10 and 6 rpm) respectively, by using a DC motor to avoid the drilling effect. The chamber of substrate and target holder evacuated to 1*10^{-3} mbar and to 1 mbar by exposing oxygen gas [19], as shown in Figure 1.

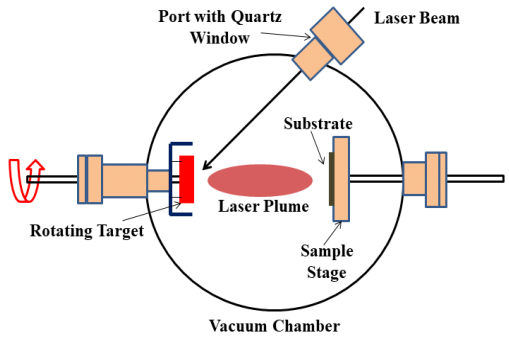

Figure 1. The schematic of the pulsed laser deposition technique [19].

RESULTS AND DISCUSSION

Structural studies

The effect of distance between substrate- target on crystal structure and orientation of all the WO_3 NPs thin film by XRD patterns are investigated. In the Figure 2 at different D_{s-t} it can be indexed to the polycrystalline structure compared to JCPDS card no. 00.32.1395 monoclinic (a=7.309, b=7.522, c=7.678). The increase in the D_{s-t} in the range (0.5, 1.5, 2.5 and 3.5 cm) lead to preferential orientation (($\bar{1}12$), ($\bar{2}02$), ($\bar{1}22$)), (002), (200), (220), (122), ($3\bar{1}1$)), ($0\bar{2}1$), ($\bar{2}01$), ($1\bar{1}2$), (022), (202), ($1\bar{2}2$), (222) and ($\bar{1}21$)) diffraction peaks, respectively, as shown in Figure 2.

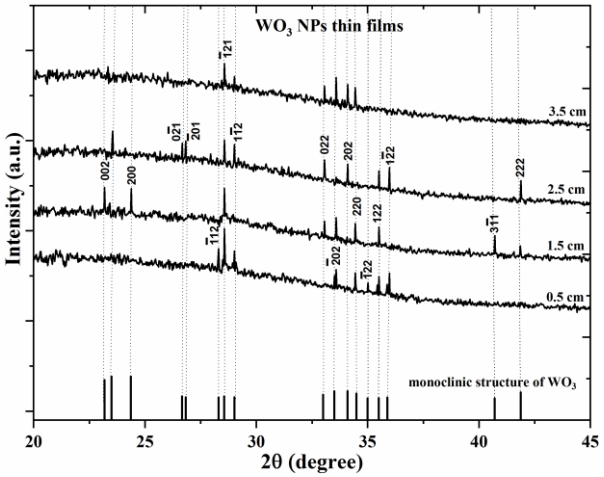

Figure 2. X-ray diffraction of WO_3 NPs thin films at the D_{s-t} (0.5, 1.5, 2.5 and 3.5 cm).

XRD investigations of WO_3 NPs has been shown that the dominant and sharp peak at 2θ =28.57 correspond to ($\bar{1}21$) plane and exhibited preferential orientation along ($\bar{1}21$) plane, as shown in Figure 3.

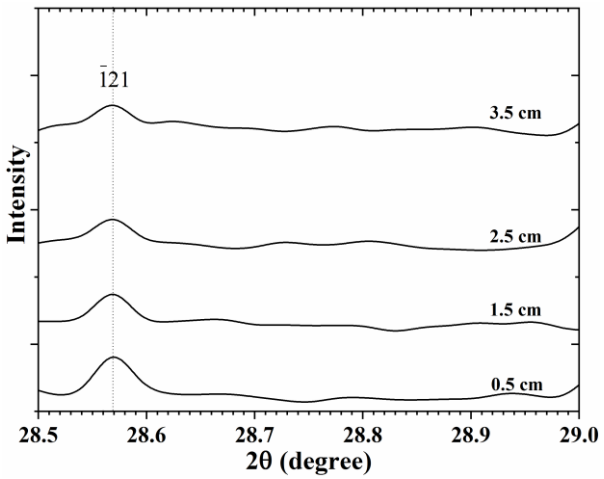

Figure 3. X-ray diffraction dominate peak of WO_3 NPs at the D_{s-t} (0.5, 1.5, 2.5 and 3.5 cm).

The intensity of ($\bar{1}21$) diffraction peak decreases with increases of D_{s-t} by 0.5, 1.5, 2.5 and 3.5 cm giving rise up decrease in the crystallite size of about 85.95, 78.63, 39.76 and 30.94 nm, respectively, due to the decrease in the thickness of WO_3 NPs thin films.

Agglomerations decrease in the form of nanoparticles were observed by SEM and average particle size distribution (D) images when the distance between the target and the substrate was increased in the range (0.5, 1.5, 2.5 and 3.5 cm) to be (163, 119, 112 and 83 nm), as shown in Figure 4: a, b, c and d, respectively.

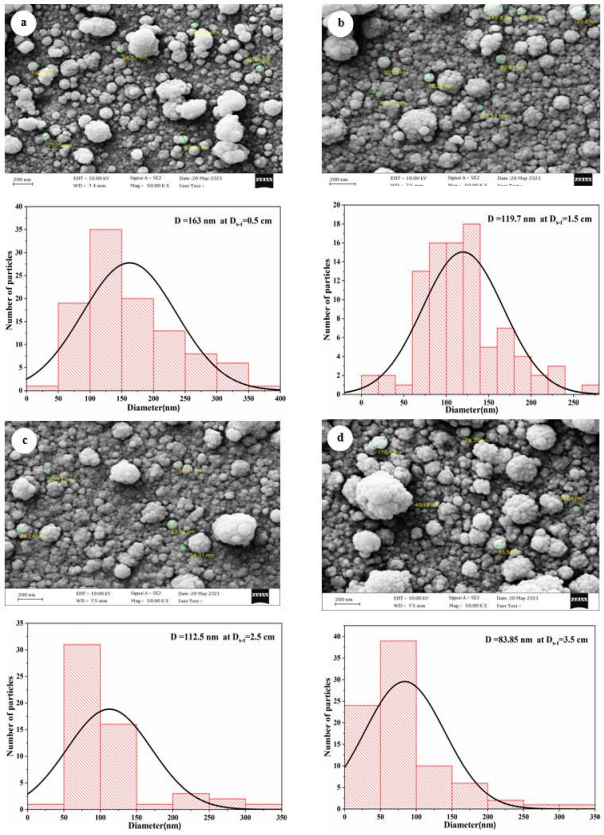

Figure 4. SEM and size distribution (D) images of WO_3 NPs: a), b), c) and d) at the D_{s-t} (0.5, 1.5, 2.5 and 3.5 cm), respectively.

The AFM images have been focused on the effect of D_{s-t} on the surface roughness of WO_3 NPs thin films, as shown in Figure 5.

When the distances between the target and the substrate are increased, the surface roughness (Sa) and RMS (Sq) of WO_3 NPs thin films definitely increase, as shown in the Table 1.

The increase of D_{s-t} leads to the increase of hemispherical expansion of the laser-induced plasma which in turn leads to an increase in the surface roughness when the substrate area at a large distance is exposed to a uniform plasma plume. Moreover, the particle flux density also increases due to the plume expansion. These high-density laser-ablated particles fast showered onto the substrate. Further, the re-sputtering of deposited material from the film surface on the shot to the shot basis of the laser beam is increased at a large target–substrate distance due to the increases in kinetic energy of the WO_3 atom [20].

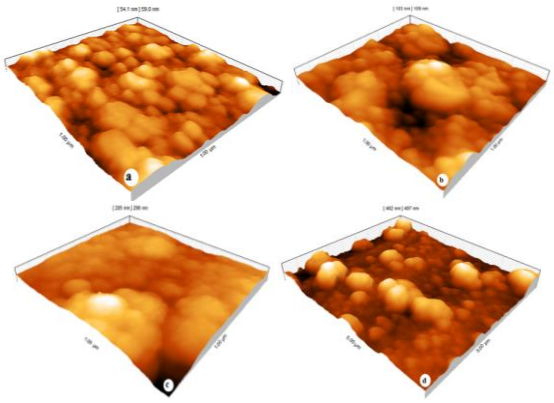

Figure 5. AFM images of WO_3 NPs thin films at the D_{s-t}: a) 0.5, b) 1.5, c) 2.5 and d) 3.5 cm.

Table 1. The roughness (Sa) and RMS (Sq) of WO_3 NPs thin films at D_{s-t} (0.5, 1.5, 2.5 and 3.5 cm).

Distance(cm)	Roughness(sa) nm	RMS (sq) nm
0.5	7.45	9.19
1.5	13.4	17.1
2.5	29.4	38.1
3.5	69.2	88.9

Optical studies

The dependence of the optical properties of WO_3 NPs thin films on the D_{s-t} was investigated by transmittance values. The fall of the light beam on the films causes an increase or decrease scattering of photons, thus affecting the values of the transmittance and absorbance of the prepared films, as shown in Figure 6.

Demonstrates the optical transmission spectra of WO_3 thin films prepared at different distances between the substrate and target that the increasing of these distances from (0.5 - 3.5 cm) lead to an increase in the transmittance and reach a maximum of 78% at the distance 3.5 cm, which shows the uniform of the prepared films and these indicate to the reduction in surface roughness is due to plume expansion [21]. The optical absorption coefficient of these films was evaluated using the relation, [22]:

$$\alpha = \frac{1}{t} ln[T/(1-R)^2] \quad (1)$$

Where T is the transmittance, R is the reflectance and t is the film thicknesses which are (153, 140, 113 and 103 nm) at the D_{s-t} (0.5, 1.5, 2.5 and 3.5 cm), respectively.

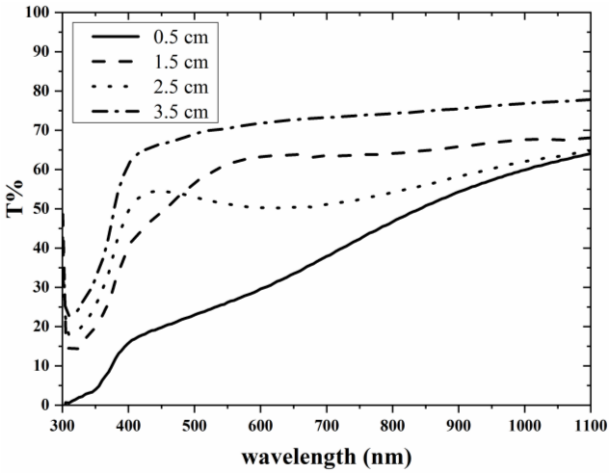

Figure 6. The transmittances of WO_3 NPs thin films at the distances (0.5, 1.5, 2.5 and 3.5 cm).

The optical absorption coefficient of WO_3 NPs thin films at the fundamental absorption edge was found to be exponentially dependent on the photon energy such that the increase of distances leads to a decrease in the values of the absorption coefficient as shown in Figure 7. The exponential dependence of the optical absorption coefficient may arise from the electronic transitions between localized states, which have tailed off in the band gap.

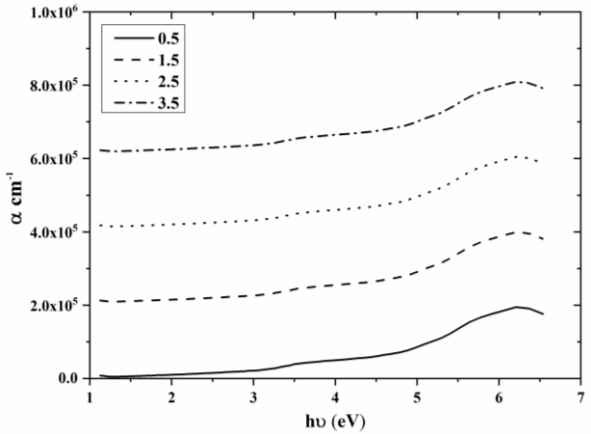

Figure 7. The absorption coefficient of WO_3 NPs films at the distance at (0.5, 1.5, 2.5 and 3.5 cm).

For incident photon energy greater than the band gap and above the exponential, the optical absorption follows a power law [23, 24]:

$$(\alpha h\upsilon) = \beta\left(h\upsilon - E_g\right)^n \qquad (2)$$

Where $h\upsilon$ is the incident photon energy, β is the edge with parameter and n is an exponent ,E_g is the optical bandgap, and α is the absorption coefficient. The exponent n determines the type of electronic transitions causing the absorption and takes the values 1/2, 3/2, 2 and 3 for direct allowed, direct forbidden, indirect allowed and indirect forbidden transitions, respectively [25,26]. The maximum values of absorbance spectra in Figure 8 at wavelengths shorter than 400 nm decrease when the distances between the substrate and target increases, as a result of the reduction of surface roughness.

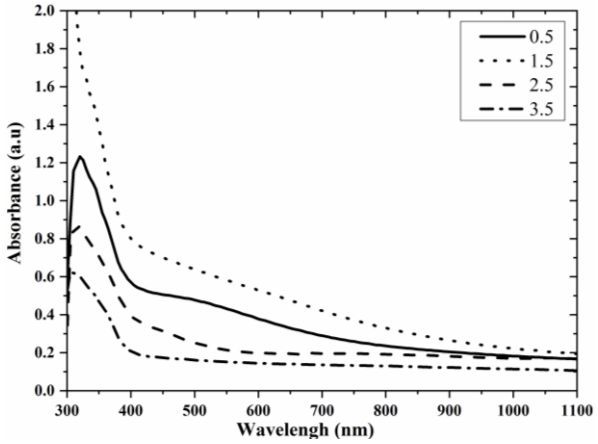

Figure 8. The absorbance spectra of WO_3NPs thin films at the distances (0.5, 1.5, 2.5 and 3.5 cm).

Thus, the optical band gap of WO_3 NPs thin films deposited at different distances determined by plotting $(\alpha h\upsilon)^{1/2}$ versus the incident photon energy (hυ), as shown in Figure 9.

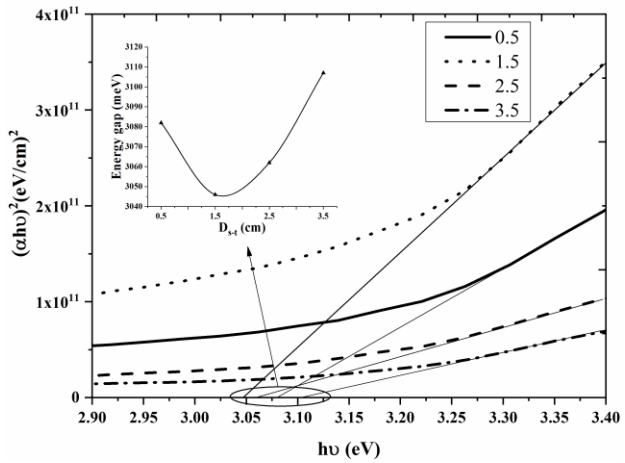

Figure 9. Energy gap (E_g) of WO_3 NPs thin films at the distances (1.5, 2.5 and 3.5 cm).

The increases in the values of energy bandgap in Figure 9 explain the effect of the increase in the substrate-target distance and which leads to a decrease in the grain size of WO_3 NPs thin films according to the quantum confinement effect. Decreasing the particle size of the prepared WO_3 thin films leads to an increase in the surface reaction of the films [27].

CONCLUSIONS

The regulation of substrate-target distance gives several indications when to prepare WO_3 NPs thin films. The optimum substrate-target distance is 2.5 cm such that the absorbance at the maximum value in the UV region gives the possibilities to use films as window device applications. At the distances of 0.5 and 1.5 cm all the UV-Visible spectrum absorbed in this region, so it can be used for solar cell applications. Also, at the distance 3.5 cm, the prepared films of WO_3 NPs can be employed in the field of gas sensors, due to the high surface roughness.

ACKNOWLEDGMENT

This work was done with the possibilities available in the thin film laboratory of the Physics Department at the Faculty of Science, Mustansiriyah University, Baghdad, Iraq.

REFERENCES

[1] M. Ahsan, T. Tesfamichael, M. Ionescu, J. Bell, N. Motta, Sens. Actuators B –Chem. 162 (2012) 14–21.

[2] X. Dong, Y.J. Gan, Y. Wang, S.J. Peng, L. Dong, J. Alloys Comp. 581 (2013) 52–55.

[3] P.J. Barczuk, A. Krolikowska, A. Lewera, K. Miecznikowski, R. Solarska, J. Augustynski, Electrochim. Acta 104 (2013) 282–288.

[4] M. Vasilopoulou, L.C. Palilis, D.G. Georgiadou, A.M. Douvas, P. Argitis, S. Kennou, L. Sygellou, G. Papadimitropoulos, I. Kostis, N.A. Stathopoulos, D.Davazoglou, Adv. Funct. Mater. 21 (2011) 1489–1497.

[5] J. Meyer, S. Hamwi, S. Schmale, T. Winkler, H.H. Johannes, T. Riedl, W.Kowalsky, J. Mater. Chem. 19 (2009) 702–705.

[6] R. Sivakumar, A. Moses Ezhil Raj, B. Subramanian, M. Jayachandran, D.C. Trivedi, C. Sanjeeviraja, Mater. Res. Bull. 39 (2004) 1479–1489.

[7] Z. Silvester Houweling, John W. Geus, Michiel de Jong, Peter-Paul R.M.L. Harks, Karine H.M. van der Werf, Ruud E.I. Schropp, Mater. Chem. Phys. 131 (2011)375–386.

[8] K.J. Lethy, D. Beena, R.V. Kumar, V.P.M. Pillai, V. Ganesan, V. Sathe, Appl. Surf. Sci. 254 (2008) 2369–2376.

[9] L.M. Bertus, C. Faure, A. Danine, C. Labrugere, G. Campet, A. Rougier, A. Duta, Mater. Chem. Phys. 140 (2013) 49–59.

[10] W.L. Kwong, N. Savvides, C.C. Sorrell, Electrochim. Acta 75 (2012) 371–380.

[11] B. Ingham, S.V. Chong, J.L. Tallon, Curr. Appl. Phys. 4 (2004) 202–205.

[12] N. Naseri, H. Kim, W. Choi, A.Z. Moshfegh, Int. J. Hydrogen Energy 38 (2013) 2117–2125.

[13] C.V. Ramana, G. Baghmar, E.J. Rubio, M.J. Hernandez, ACS Appl. Mater. Int. 5 (2013) 4659–4666.

[14] S. Keshri, A. Kumar, D. Kabiraj, Thin Solid Films 526 (2012) 50–58.

[15] N. J. Mohammed, S. S. Hamod, "Substrate temperature dependence of optical and morphological properties of ZnTe nanoparticles thin films," Journal of College of Education, vol. 1, no. 1, pp. 101-118, 2019.

[16] N. J. Mohammed, H. A. Ahmed, "Effect of Laser Fluence on Structural Transformations and Photoluminescence Quenching of Zinc Selenide Nanoparticles Thin Films," Al-Mustansiriyah Journal of Science, vol. 29, no. 4, pp. 122-127, 2019.

[17] K.J. Lethy, D. Beena, R.V. Kumar, V.P.M. Pillai, V. Ganesan and V. Sathe, Structural, optical andmorphological studies on laser ablated nano structured WO3 thin films, Appl. Surf. Sci. 254 (2008)2369.

[18] S. Yamamoto, A. Inouye and M. Yoshikawa, Structural and gasochromic properties of epitaxial WO3films prepared by pulsed laser deposition, Nucl. Instrum. Meth. B 266 (2008) 802.

[19] A.Z. Mohammed, N.J. Mohammed, I.K. Khudhair, "Effect of the Number Shots of Laser on Structural Transformations and Optical Properties of ZnS Nanoparticles Thin Films," Arab J. Nucl. Sci. Appl., vol. 51, 4, pp. 108-117, 2018.

[20] J.M. Warrender, M.J. Aziz,. Kinetic energy effects on morphology evolution during pulsed laser deposition of metal-on-insulator films. Phys. Rev., B 75(8): 085433-085444, 2007

[21] K. J. Chopra, Thin film Phenomena, Mc Graw-Hill, New yark, 1969, p. 734.

[22] K.J.Patel, C.J.Panchal, V.A.Kheraj, M.S.Desai, Materials Chemistry and physics. 114(2009) 475-478.

[23] N. Kenny, C.R. Kannewurt, S. H. Whitemore, J. Phys, Chem. Solids. 27 (1966) 1237.

[24] E. A. Davis, N. F. Mott, Phil. Mag. 22 (1970) 903.

[25] J. Tauc, R. Grigo Rovici, A. Vancu, Phys. Status Solidi 15 (1966) 627–637.

[26] Ho SM, SA V, Ahmed G, Vidya NS. A review of nanostructured thin films for gas sensing and corrosion protection. Mediterranean Journal of Chemistry. 2018 Jun 1;7(6).

[27] Prajapati, C.S.; Bhat, N. ppb level detection of NO2 using a WO3 thin film-based sensor: Material optimization, device fabrication and packaging. RSC Adv. 2018, 8, 6590–6599.